Section 9

Development of and studies with coupled and Earth system models and data assimilation systems.

Diagnosing the ocean-atmosphere coupling schemes by using a mathematically consistent Schwarz iterative method

Olivier Marti[1], Sébastien Nguyen[1], Pascale Braconnot[1], Sophie Valcke[2], Florian Lemarié[3], and Eric Blayo[3]

[1]Laboratoire des Sciences du Climat et de l'Environnement, LSCE/IPSL, CEA-CNRS-UVSQ, Université Paris-Saclay, Gif-sur-Yvette, France
[2]CECI, Université de Toulouse, CNRS, CERFACS, Toulouse, France
[3]Univ. Grenoble Alpes, Inria, CNRS, Grenoble INP, LJK, 38000, Grenoble, France
Correspondence: olivier.marti@lsce.ipsl.fr

1 Introduction

Coupling algorithms implemented in coupled general circulation models (CGCMs) are driven by the necessity to conserve energy and mass at the air-sea interface. The discretization of the coupling problem leads to inconsistencies in time. It splits the simulation into small time intervals (coupling periods) over which averaged-in-time boundary data are exchanged. Atmosphere computes the fluxes at the interface (heat, water and momentum), and ocean computes the sea surface properties (water and sea ice temperatures, sea ice fraction, albedos, surface current). Two main algorithms are used, the *parallel* and the *sequential atmosphere-first*. In the *parallel* algorithm, both models run a coupling period with the boundary conditions of the other model from the previous coupling period. In the *sequential atmosphere-first* algorithm, atmosphere runs with oceanic boundary conditions from the previous coupling time. Then ocean runs with atmospheric boundary conditions of the current coupling period. Both algorithms are lagged: there is a time lag (of one coupling period) between the model and its boundary conditions, for one (*sequential* algorithm) or both (*parallel* algorithm) models.

Schwarz algorithms are attractive iterative coupling methods to cure the temporal inconsistencies and provide tightly and mathematically consistent coupled solutions. As discussed in Lemarié (2008), the standard coupling methods correspond to one single iteration of a global-in-time iterative Schwarz method.

2 The Schwarz iterative method

A Schwarz iterative method has been implemented in the IPSLCM5A Earth System model (Sepulchre et al., 2020; Marti et al., 2010, 2021). The model repeats each coupling period, with the same initial state (the result from the previous coupling period). The boundary conditions are updated at each iteration, using the result of the previous iteration, until convergence. The solution is mathematically consistent: during a coupling period, each model uses the boundary conditions from the other model for the same coupling period. There is no lag.

The method has a huge computational cost, as each coupling period is iterated. It is not affordable for production runs, but allows us to compare the legacy coupling algorithms used in state-of-the art GCM to a mathematically consistent and synchronous algorithm, which is used as a reference to compute the error made with legacy algorithms.

We run 5-day experiments with the Schwarz iterative method, using three algorithms (*parallel*, *sequential atmosphere-first* and *sequential ocean-first*), and two coupling periods $\Delta t = 1h$ and $\Delta t = 4h$. The Schwarz method can be used over all these algorithms. If the method is run until perfect convergence, the result is not dependant of the underlying coupling algorithm. In practice, the iterative method will be stopped before perfect convergence with an ad hoc criterion, and the different algorithms will give slightly different results.

3 Results

Fig. 1 shows the relative error in the change of sea surface temperature (SST) during one coupling period when the Schwarz method is not used. At each Schwarz iteration, the model computes an occurrence of the SST trend. At the first iteration, the trend is the one that the model would calculate with the legacy lagged coupling. It is compared with the trend obtained after convergence. The comparison is done on a unique trajectory of the model. The error is computed as the ratio between the correction due to the iterative procedure and the solution change with no Schwarz iteration. We consider each case of the iterative process, i.e. each point of the atmosphere grid, and for each coupling period.

In the *parallel*-$\Delta t = 1h$ experiment, the relative error is negligible (less than 0.01) in about 15 % of the cases. It is small (less than 0.1) in almost 50 % of the

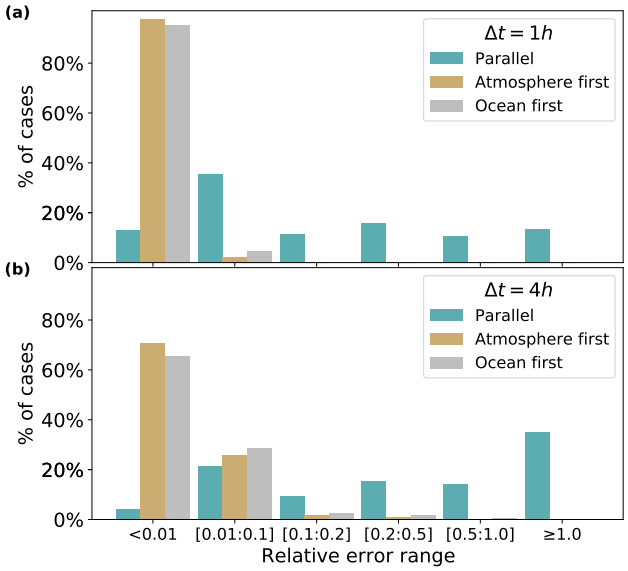

Figure 1: Relative error of the change of sea surface temperature during a coupling period. The error is computed as the ratio between the correction due to the iterative procedure and the solution change during a coupling period with no Schwarz iteration. The ordinates show the number of cases in percentage of the total number of cases in *time* × *space*.

cases. But it is larger than 0.1 for the other half. The relative error is even larger than 0.5 in 25 % of the cases. The *atmosphere-first* shows strongly improved results, with a negligible error for 97 % of the points. The results of the *ocean-first* experiment are close to the *atmosphere-first* experiments, with a slight deterioration. For the $\Delta t = 4h$ experiments, the errors are larger than in the $\Delta t = 1h$ case, but with the same hierarchy between the algorithms.

The error shows a strong diurnal cycle (not shown) with the lowest errors during the night. Errors are larger at noon than at midnight. The error is maximum after sunset and before sunrise, when the change of the insolation forcing evolves at the fastest pace.

We propose two hypotheses to explain the *atmosphere-first* algorithm performance compared to *ocean-first*. First, the atmosphere has shorter characteristic time scales than the ocean, with a more marked diurnal cycle. The atmospheric lower boundary conditions evolves slowly, and the atmospheric solution after the first half-iteration is then already quite close to its converged value, and provides a relevant and synchronized forcing to compute the oceanic solution in the second half-iteration. Second, the better performance of the *atmosphere-first* case can also be linked to the phasing of the solar radiation, which is the only external forcing and constrains the diurnal cycle. In the *ocean-first* case, the ocean is forced by fluxes, including solar radiation, calculated by the atmosphere at the previous coupling period. For *atmosphere-first*, the solar forcing is correctly phased.

Most current GCMs use the *parallel* algorithm which appears to have very large errors (see Marti et al. (2021) for a short review). Our analysis shows that implementing *sequential* algorithms are simple ways to strongly reduce the error, with the *atmosphere-first* algorithm showing the best performance. The *sequential* algorithms, however, have a major drawback. The models do not run concurrently as, while one model is running, the other model waits for its boundary conditions. This eliminates a level of parallelism, and increases the time to solution of the coupled model.

4 Acknowledgements

This study is part of the ANR project COCOA (`https://anr.fr/Projet-ANR-16-CE01-0007`). This work was granted access to the HPC resources of TGCC under an allocation made by GENCI (Grand équipement National de Calcul Intensif, grant 2019-A0040100239). It benefits from the development of the common modelling IPSL infrastructure coordinated by the IPSL climate modeling center (`https://cmc.ipsl.fr`).

References

Lemarié, F. (2008). *Algorithmes de Schwarz et couplage océan-atmosphère*. PhD thesis, Université Joseph Fourier, Grenoble.

Marti, O., Braconnot, P., Dufresne, J.-L., Bellier, J., Benshila, R., Bony, S., Brockmann, P., Cadule, P., Caubel, A., Codron, F., de Noblet, N., Denvil, S., Fairhead, L., Fichefet, T., Foujols, M.-A., Friedlingstein, P., Goosse, H., Grandpeix, J.-Y., Guilyardi, E., Hourdin, F., Idelkadi, A., Kageyama, M., Krinner, G., Lévy, C., Madec, G., Mignot, J., Musat, I., Swingedouw, D., and Talandier, C. (2010). Key features of the IPSL ocean atmosphere model and its sensitivity to atmospheric resolution. *Clim. Dyn.*, 34(1):1–26.

Marti, O., Nguyen, S., Braconnot, P., Valcke, S., Lemarié, F., and Blayo, E. (2021). A Schwarz iterative method to evaluate ocean- atmosphere coupling schemes. Implementation and diagnostics in IPSL-CM6-SW-VLR. *Geosci. Model Dev. Discuss.*, 2021:1–19.

Sepulchre, P., Caubel, A., Ladant, J.-B., Bopp, L., Boucher, O., Braconnot, P., Brockmann, P., Cozic, A., Donnadieu, Y., Dufresne, J.-L., Estella-Perez, V., Ethé, C., Fluteau, F., Foujols, M.-A., Gastineau, G., Ghattas, J., Hauglustaine, D., Hourdin, F., Kageyama, M., Khodri, M., Marti, O., Meurdesoif, Y., Mignot, J., Sarr, A.-C., Servonnat, J., Swingedouw, D., Szopa, S., and Tardif, D. (2020). IPSL-CM5A2 – an Earth system model designed for multi-millennial climate simulations. *Geophys. Res. Lett.*, 13(7):3011–3053.

Numerical simulations of the rapid weakening of Typhoon Haishen (2020) by a coupled atmosphere-wave ocean model

Akiyoshi Wada and Wataru Yanase

[1]Meteorological Research Institute, Tsukuba, Ibaraki, 305-0052, JAPAN

[1]awada@mri-jma.go.jp

1. Introduction

Wada (2021) investigated the effect of the ocean on Typhoon Haishen (2020) using the results of numerical simulations conducted by a nonhydrostatic atmosphere model (NHM) and the coupled atmosphere-wave-ocean model (CPL, Wada, et al., 2018). Wada (2021) concluded that the simulation result by CPL with the KF cumulus parameterization seems to be better for the intensity change in the weakening phase. In fact, Haishen was a relatively compact typhoon with a concentric eyewall. Haishen had a multiple eyewall structure at 15 UTC on 5 September (Fig. 1a) in the mature phase, but the innermost eyewall collapsed at 03 UTC on 6 September (Fig. 1b) in the weakening phase.

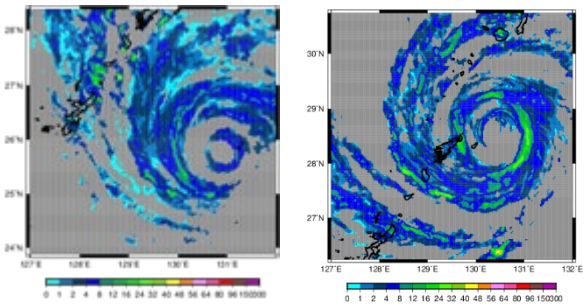

Figure 1 The 1-hour rainfall distribution analyzed every 5 minutes (mm/hour) at (a) 15 UTC on 5 September and (b) 03 UTC on 6 September.

To investigate the effect of the ocean coupling and sea surface temperature (SST) at the initial integration time on the inner-core structural change and thereby intensity change of Haishen, numerical simulations were conducted by using the 1-km mesh NHM and CPL.

2. Experimental design

Table 1 shows a list of numerical simulations. The initial time of integration was 0000 UTC on 5 September. The computational domain was 1500 x 2040 km with a grid spacing of 1 km. The number of the vertical layer was 50. The top height was approximately 21 km. The integration time was 48 hours. The cumulus parameterization of Kain and Fritsch (1990) (KF in Table 1) was used for comparison.

Table1 List of numerical simulations

Name	*Model*	*SST at the initial time*	*Cumulus Parameterization*
NHMKF	NHM	OISST on 5 September	Kain and Fritsch (1990)
CPLKF	CPL	OISST on 5 September	Kain and Fritsch (1990)
NHMKF3DB	NHM	OISST on 2 September	Kain and Fritsch (1990)
CPLKF3DB	CPL	OISST on 2 September	Kain and Fritsch (1990)

The time step was 1 second for NHM, 6 seconds for the ocean model, and 6 minutes for the ocean surface wave model. The Japan Meteorological Agency (JMA) mesoscale objective analysis with horizontal resolution of 5 km and the JMA North Pacific Ocean analysis with horizontal resolution of 0.5° were used for creating atmospheric and oceanic initial conditions and atmospheric lateral boundary conditions (every 3 hours). As for the initial condition of SST, the Optimally Interpolated SST (OISST) daily product with horizontal resolution of 0.25°, obtained from the site: http://www.remss.com, was used. The dates of OISST used to create the initial condition of SST are not only 5 September but also 2 September (3DB, see Table 1).

3. Results

3.1 Simulated track and intensity

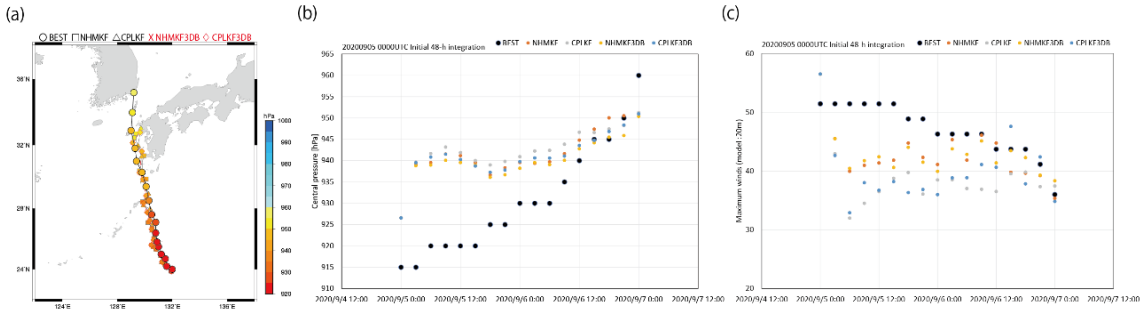

Figure 2 (a) Simulated tracks together with the Regional Specialized Meteorological Center (RSMC) Tokyo best track. (b) Simulated central pressures together with the RSMC best track central pressure. (c) Simulated maximum wind speeds at the height of 20 m together with the RSMC best track maximum wind speed at the height of 10 m. The interval of plots is 3 hours.

Figure 2a shows the results of track simulations together with the Regional Specialized Meteorological Center

(RSMC) Tokyo best track (https://www.jma.go.jp/jma/jma-eng/jma-center/rsmc-hp-pub-eg/besttrack.html). All simulated tracks are reasonable to the best track although the moving speed of simulated Haishen is relatively slow. There is no impact of ocean coupling and different SST distribution at the initial time on the track simulation. Figures 2b and 2c show the result of Haishen's intensity simulations. Differently from the result in the intensification phase (Wada, 2021), there is less impact of ocean coupling and different SST distribution at the initial time on the simulated central pressures (Fig. 2b). However, the effect of ocean coupling on the simulated maximum wind speed is obvious (Fig. 2c). In other words, a simulated wind-pressure relationship is changed due to ocean coupling.

3.2 SST and Inner-core structural change

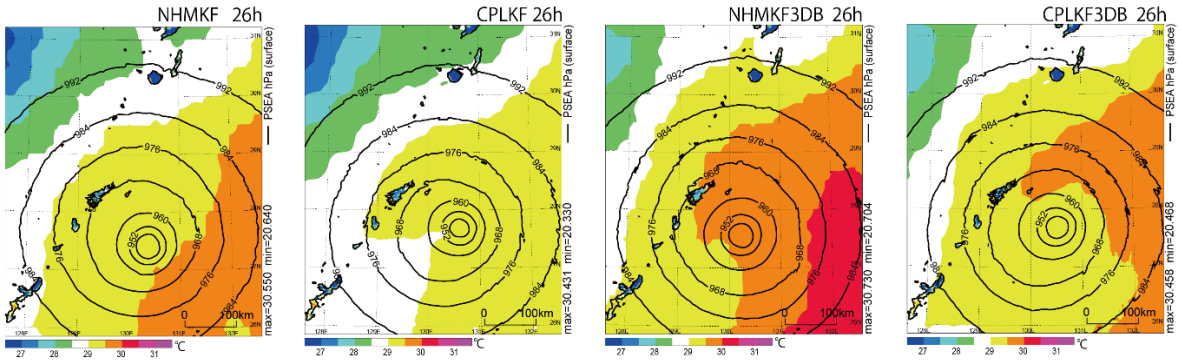

Figure 3 The horizontal distribution of SST in the experiments NHMKF, CPLKF, NHMKF3DB and CPLKF3DB at the 26-h integration time.

Figure 3 shows the horizontal distribution of SST at the 26-h integration time in the experiments NHMKF, CPLKF, NHMKF3DB and CPLKF3DB. In the experiments NHMKF and NHMKF3DB, the SST distribution is fixed during the integration. In the experiments CPLKF and CPLKF3DB, sea surface cooling is simulated by the passage of simulated Haishen. However, the SST in the vicinity of the center of Haishen keeps 29~30 ˚C at the 26-h integration time in all experiments.

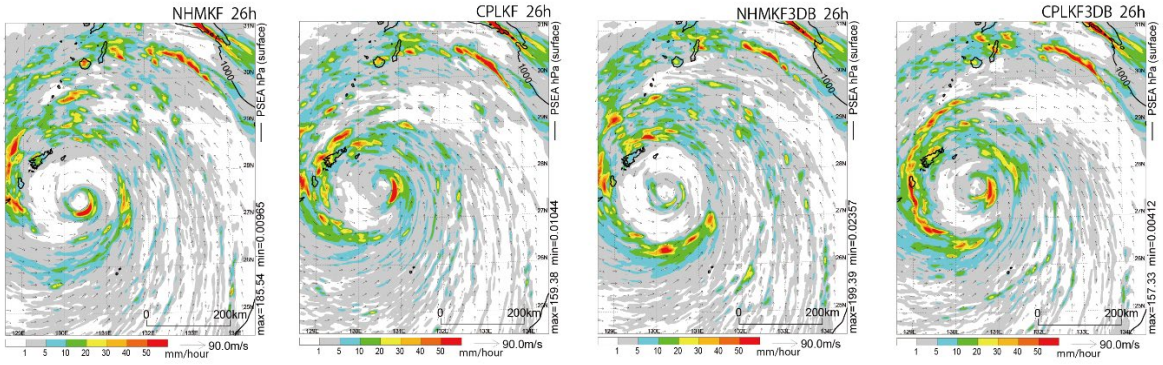

Figure 4 The horizontal distribution of hourly rainfall (shades), sea-level pressure (contours) and surface winds (vectors) in the experiments NHMKF, CPLKF, NHMKF3DB and CPLKF3DB at the 26-h integration time.

Figure 4 shows the horizontal distribution of hourly precipitation around the center of simulated Haishen at the 26-h integration time in the experiments NHMKF, CPLKF, NHMKF3DB and CPLKF3DB. Concentric eyewall in the vicinity of the center of simulated Haishen is clearly simulated at the 26-h integration time in the experiments NHMKF and NHMKF3DB. However, the innermost eyewall collapses at the 26-h integration time in the experiments CPLKF and CPLKF3DB. The result suggests that ocean coupling may be related to the corruption of the innermost eyewall as is shown in Fig. 1b. In addition, the difference in the initial SST distributions also affects the distribution of hourly precipitation particularly in the outer concentric rainband even though the impact of the simulated central pressure is small.

4. Concluding remarks

The 1-km mesh atmosphere-wave-ocean coupled-model simulation with KF cumulus parameterization enables to simulate a multiple eyewall structure and the corruption of the innermost eyewall in the case of Haishen. However, the result of intensity simulation is not realistic. To simulate more accurate intensity of Haishen, the simulation at an earlier integration time should be improved. The model top height (~21km) may be too low for Haishen.

References

Kain, J. S., and J. M. Fritsch (1990). A one-dimensional entraining/detraining plume model and its application in convective parameterization. Journal of the Atmospheric Sciences, 47, 2784-2802.

Wada, A. (2021). Numerical simulations of Typhoon Haishen by a coupled atmosphere-wave ocean model with two different oceanic initial conditions. Research Activities in Earth System Modelling, Submitted.

Wada, A., S. Kanada, and H. Yamada (2018). Effect of air–sea environmental conditions and interfacial processes on extremely intense typhoon Haiyan (2013). Journal of Geophysical Research: Atmospheres, 123, 10379-10405.

Atmosphere-wave-ocean coupled-model ensemble simulation on rapid intensification of Typhoon Hagibis (2019)

Akiyoshi Wada

[1]Meteorological Research Institute, Tsukuba, Ibaraki, 305-0052, JAPAN

[1]awada@mri-jma.go.jp

1. Introduction

Wada (2020) reported from the results simulated by a 1-km mesh nonhydrostatic atmosphere model and the coupled atmosphere-wave-ocean model (Wada et al., 2018) that the rapid intensification and the sustenance of the lowest central pressure of Hagibis (2019) occurred when it passed over the ocean where the upper-ocean heat content was higher than the climatological mean. Regarding the impact of a difference in the oceanic initial conditions between real-time daily analysis and climatological daily mean on the simulated central pressure of Hagibis in the intensification phase, the central pressures simulated with the oceanic initial condition obtained from the real time oceanic daily analysis dataset tended to be lower than those obtained from the climatological daily mean. This result, however, is obtained from a single deterministic simulation result at one specific atmospheric initial condition and thus it is not always robust for various atmospheric initial conditions. To perform an ensemble simulation for Hagibis, multiple atmospheric initial conditions are needed. This report conducts two sets of ensemble simulation by using the results of ensemble simulations conducted by the coupled atmosphere-wave-ocean model with two different oceanic initial conditions and focuses on the difference in the impact of a difference in the oceanic initial conditions on simulated Hagibis in the intensification phase.

2. Experimental design

The experimental design is the same as Wada (2020). The atmospheric initial condition in Wada (2020) is regarded as that in the control run. The Japan Meteorological Agency (JMA) global atmospheric ensemble prediction data with a horizontal grid spacing of 1.25° were used to add perturbations to the atmospheric initial condition used in Wada (2020). Although up to 50 perturbations were available, 25 of them were used in this study due to the limitation of computational resources. Two sets of ensemble simulation were carried out using these 26 atmospheric initial conditions for the real time and climatological mean oceanic initial conditions, respectively. The integration time in all simulations was 48 hours. However, the simulation of one atmospheric initial condition (No.19) with the climatological mean oceanic initial condition became unstable during the integration and terminated abnormally. This is the reason that the analysis period is from the initial time up to 36 hours. The Regional Specialized Meteorological Center (RSMC) Tokyo best track data is used for validation of the simulation results.

3. Results

3.1 Simulated track and central pressure

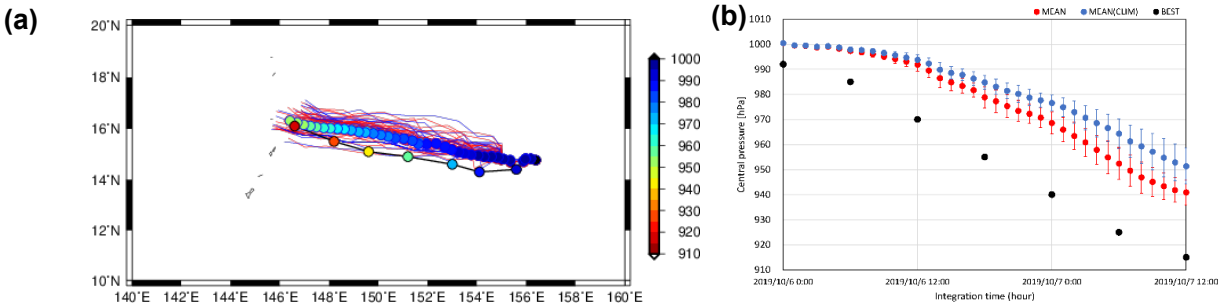

Figure 1 Results of (a) ensemble mean track simulations (a line with circles every hour) and (b) ensemble mean central pressures with the standard deviation every hour. Red colors in Figs. 1a, b show the results of numerical simulations with the real time oceanic initial condition, while blue colors in Figs. 1a, b show those with the climatological mean oceanic initial condition. Black colors in Figs. 1a, b show the RSMC best track (data is depicted every 6 hours). Colors within the circle in Fig. 1a shows the value of central pressure (The unit of the color bar is hPa).

Figure 1a shows a simulated track in each member, the ensemble mean simulated with the real time oceanic initial condition and the ensemble mean with the climatological mean oceanic initial condition, and the RSMC best track for validation. Each simulated track and the ensemble mean were deflected north irrespective of the oceanic initial condition, which is the same as the result of Wada (2020). The width of the ensemble spread normal to the track of ensemble mean (Fig. 1a) shows that the northward bias cannot be improved by simply replacing the atmospheric initial condition. This suggests that it is necessary to set a larger number of ensemble members to statistically improve the track simulation. Nevertheless, it should be noted that a few simulated tracks are close to the RSMC best track or shows the southward deflection compared to the RSMC best track.

Figure 1b shows the time series of the ensemble mean central pressures simulated with the real time oceanic initial

condition, those simulated with the climatological mean oceanic initial condition and the RSMC best track central pressure. The standard deviation is calculated for simulated central pressures every hour. The initial value of center pressure used in the ensemble simulations is higher than that of RSMC best track central pressure irrespective of the addition of the perturbation to the atmospheric initial condition. Regarding the impact of difference in the oceanic initial conditions between real-time analysis and climatological mean on the central pressure simulation, the central pressures simulated with the real time oceanic initial condition tend to be lower than those simulated with the climatological mean oceanic initial condition. The difference of simulated central pressures between the real time and the climatological mean oceanic initial conditions is significant after 07 UTC on 6 September (after the 7-hour integration time) at the 99% confidence level based on t-test. The result supports the findings of Wada and Chan (2021) that Hagibis became stronger because the amount of the upper ocean heat content (tropical cyclone heat potential) increased recently around 15-20°N, 140-150°E.

3.2 Sea surface temperature distribution

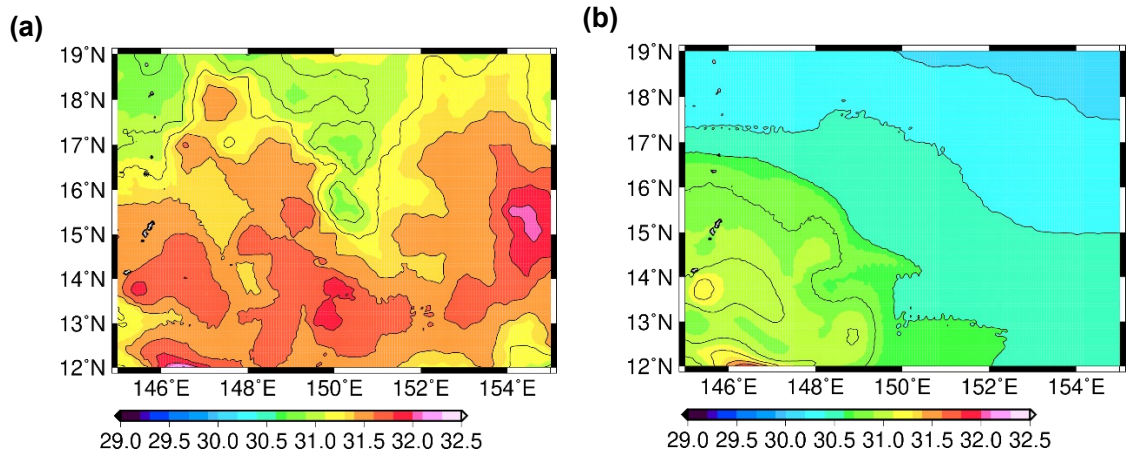

Figure 2 Horizontal distributions of the ensemble mean SST (°C) simulated with (a) the real time oceanic initial condition and that simulated with (b) the climatological mean oceanic initial condition. The contour interval is 0.1°C. Colors also indicate the value of SST.

Figure 2 shows the horizontal distributions of ensemble mean sea surface temperature (SST) at the 36-h integration time simulated with the real time oceanic initial condition (Fig. 2a) and with the climatological mean oceanic initial condition (Fig. 2b), respectively. The ensemble mean SST simulated with the real oceanic initial condition is higher in the whole computational domain than that simulated with the climatological mean. It is considered that the difference in the ensemble mean of simulated SST is related to that in simulated central pressure of approximately 10 hPa shown in Fig. 1b, which corresponds to the result of Wada and Chan (2021). Despite the clear difference in the ensemble mean of simulated SST distribution shown in Fig. 2, however, the impact on the ensemble mean of simulated Hagibis's track is small. It should be noted that the atmospheric initial condition used in this study is the same in the two sets of ensemble experiments, which does not reflect the difference in the atmosphere resulted from the difference in the oceanic initial condition or the difference due to the recent upper-ocean warming (Wada and Chan, 2021).

4. Summary and future subject

This study focused on the effect of the difference in the oceanic initial conditions between real-time analysis and climatological mean on the simulation of Typhoon Hagibis (2019) in the intensification phase. Two sets of ensemble simulations are performed separately with a 1-km mesh regional atmosphere-wave-ocean coupled model and 26 atmospheric initial conditions created by adding the perturbation based on JMA global atmospheric ensemble prediction data. The result shows that the difference of simulated central pressures between real-time analysis and climatological mean oceanic initial conditions is significant after the 7-hour integration time at the 99% confidence level based on t-test although there is little impact on the ensemble mean of simulated tracks. The difference in the ensemble mean of simulated SST is related to that in simulated central pressure of approximately 10 hPa at the 36-h integration time, which is consistent with the result of Wada and Chan (2021). It is one of the subjects in the future that the effect of ocean coupling on the ensemble simulation with 26 atmospheric initial conditions will be statistically investigated by conducting another ensemble simulation with a noncoupled atmosphere model.

References

Wada, A., S. Kanada, and H. Yamada (2018). Effect of air–sea environmental conditions and interfacial processes on extremely intense typhoon Haiyan (2013). Journal of Geophysical Research: Atmospheres, 123, 10379-10405.

Wada, A., (2020). Atmosphere-wave-ocean coupled-model simulation on rapid intensification of Typhoon Hagibis (2019). Research Activities in Earth System Modelling, Working Group on Numerical Experimentation. Report No.50, WCRP Report No.12/2020. WMO, Geneva, p. 9 -15.

Wada, A., and J. C. L. Chan, (2021). Increasing TCHP in the western North Pacific and its influence on the intensity of FAXAI and HAGIBIS in 2019. SOLA, 17A, 29-32.

Numerical simulations of Typhoon Haishen by a coupled atmosphere-wave ocean model with two different oceanic initial conditions

Akiyoshi Wada and Wataru Yanase

[1]Meteorological Research Institute, Tsukuba, Ibaraki, 305-0052, JAPAN

[1]awada@mri-jma.go.jp

1. Introduction

A tropical depression was upgraded to a tropical storm around 22.6°N, 145.9°E at 12 UTC on 31 August in 2020, which was named Haishen. Haishen moved southwestward in the early intensification phase and then changed the direction to northwestward from 2 September. During the northwestward movement in the intensification phase, Haishen reached the minimum central pressure of 910 hPa at 12 UTC on 4 September. On 5 September, Haishen changed the direction to north northwestward and entered the East China Sea on 6 September. The Japan Meteorological Agency (JMA) forecasted that Haishen would be extremely strong (below 930 hPa) in the East China and possibly make landfalling in Japan while sustaining the strong intensity. However, Haishen weakened rapidly before entering the East China Sea. In the East China Sea, sea surface cooling was caused by the passage of preceding typhoon, Maysak. However, the cold wake was not sufficiently analyzed in the oceanic initial condition used in the forecast. To investigate the effect of the sea surface temperature (SST) distribution at the initial time and ocean coupling processes on the rapid weakening of Haishen, numerical simulations were conducted by using a nonhydrostatic atmosphere model (NHM) and the coupled atmosphere-wave-ocean model (CPL) (Wada et al., 2018).

2. Experimental design

Table 1 shows a list of numerical simulations. Each initial time was 0000 UTC on 2 September in 2020. The computational domain was 3080 x 3480 km with a grid spacing of 2 km. The number of the vertical layer was 55. The top height was approximately 27 km. The integration time was 132 hours. The time step was 5 seconds for NHM, 30 seconds for the ocean model, and 6 minutes for the ocean surface wave model. The cumulus parameterization of Kain and Fritsch (1990) (KF in Table 1) was used for comparison.

Table1 List of numerical simulations

Name	*Model*	*SST at the initial time*	*Cumulus Parameterization*
NHM	NHM	OISST	-
CPL	CPL	OISST	-
NHM_MGD	NHM	MGDSST	-
CPL_MGD	CPL	MGDSST	-
NHMKF	NHM	OISST	Kain and Fritsch (1990)
CPLKF	CPL	OISST	Kain and Fritsch (1990)
NHMKF_MGD	NHM	MGDSST	Kain and Fritsch (1990)
CPLKF_MGD	CPL	MGDSST	Kain and Fritsch (1990)

The JMA global objective analysis with horizontal resolution of 20 km and the JMA North Pacific Ocean analysis with horizontal resolution of 0.5° were used for creating atmospheric and oceanic initial conditions and atmospheric lateral boundary conditions. As for the initial condition of SST, the Optimally Interpolated SST (OISST) daily product with horizontal resolution of 0.25°, obtained from the Remote Sensing Systems (http://www.remss.com) was used. In addition, the Merged satellite and in situ data Global Daily Sea Surface Temperatures in the global ocean (MGDSST) data set (Kurihara et al., 2006) (MGD in Table 1) was used for comparison.

3. Results

3.1 Track simulations

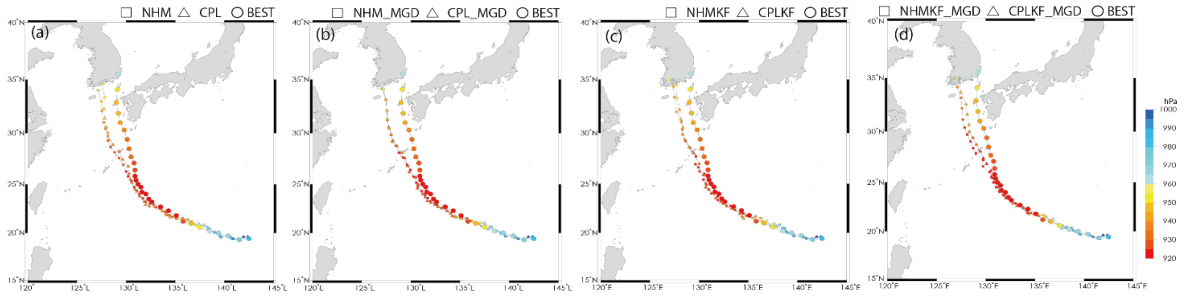

Figure 1 Simulated tracks in the experiments (a) NHM and CPL, (b) NHM_MGD and CPL_MGD, (c) NHMKF and CPLKF, and (d) NHMKF_MGD and CPLKF_MGD together with the RSMC best track. The interval is 3 hours for simulation results, while that is 3 or 6 hours depending on the location of Haishen relative to the Japanese archipelago. Colors in marks indicate the value of central pressure.

Figure 1 shows the results of simulated tracks and central pressures in all simulations together with the Regional Specialized Meteorological Center (RSMC) Tokyo best track (https://www.jma.go.jp/jma/jma-eng/jma-center/rsmc-hp-pub-eg/besttrack.html) data. All simulated tracks clearly show a westward deflection compared to the best track after the best track Haishen changes the moving direction north-northwestward. The result indicates that there is less impact of ocean coupling and cumulus parameterization on the simulated tracks.

3.2 Intensity changes

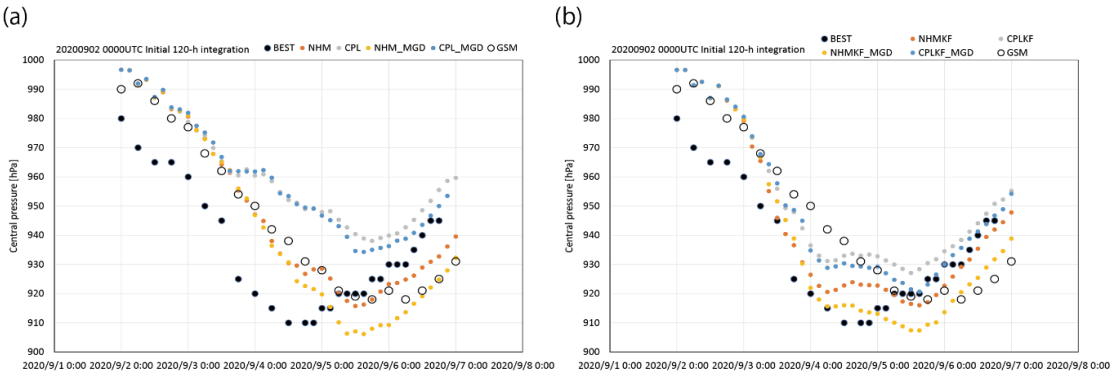

Figure 2 The evolution of RSMC best track central pressure, central pressures predicted by JMAGSM, and simulated central pressures in the experiments (a) NHM, CPL, NHM_MGD, and CPL_MGD and (b) NHMKF, CPLKF, NHMKF_MGD, and CPLKF_MGD.

Figure 2 shows the simulation results of central pressures, the prediction result of central pressures calculated by JMA global spectral model (GSM) and the RSMC best track central pressure. Since the initial value of central pressure differs between the RSMC best track central pressure and the central pressure at the initial time of integration used in all simulations and the prediction by GSM, the values of simulated central pressure and central pressure predicted by GSM tend to be higher than the best track central pressure in the intensification phase from the initial time to 00 UTC on 5 September. In addition, the time to reach the lowest central pressure, including the GSM results, is later than that of the RSMC best track. This may be one of the reasons that overdevelopment was forecasted in the East China Sea.

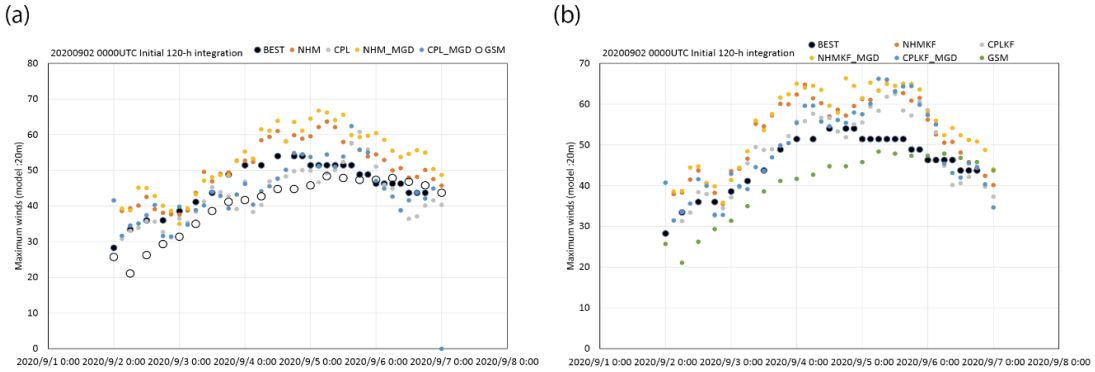

Figure 3 The evolution of RSMC best track 10-m maximum wind speed, 10-m maximum wind speeds predicted by JMA global spectral model and simulated 20-m maximum wind speeds in the experiments (a) NHM, CPL, NHM_MGD, and CPL_MGD and (b) NHMKF, CPLKF, NHMKF_MGD, and CPLKF_MGD.

Figure 3 shows the simulation results of 20-m maximum winds, the prediction result of 10-m maximum winds calculated by JMA global spectral model (GSM) and the RSMC best track 10-m maximum sustained wind speed. The height of 20 m corresponds to the model level near the surface. The effect of ocean coupling on 20-m maximum wind speed is more obvious in the experiments without the KF cumulus parameterization (NHM, CPL, NHM_MGD, and CPL_MGD) than that in the experiment with the cumulus parameterization (NHMKF, CPLKF, NHMKF_MGD, and CPLKF_MGD). Although the simulated tracks are shifted to the west, the simulation result by the coupled model with the cumulus parameterization seems to be better for the intensity change in the weakening phase, which is consistent with the result shown in Fig. 2.

4. Future study

Haishen was a relatively compact typhoon with a concentric eyewall. One of the ideas is the investigation of the effects of ocean coupling and cumulus convection on the inner-core structural change. The other idea, which will be reported in a companion report (Wada, 2021), is to investigate the effect of higher resolution (less than 1 km) on the simulation of Haishen.

References

Kain, J. S., and J. M. Fritsch (1990). A one-dimensional entraining/detraining plume model and its application in convective parameterization. Journal of the Atmospheric Sciences, 47, 2784-2802.

Kurihara, Y., T. Sakurai, and T. Kuragano (2006). Global daily sea surface temperature analysis using data from satellite microwave radiometer, satellite infrared radiometer and in-situ observations. Sokko-jiho, 73, S1-S18 (in Japanese).

Wada, A. (2021). Numerical simulations of the rapid weakening of Typhoon Haishen (2020) by a coupled atmosphere-wave ocean model. Research Activities in Earth System Modelling, WGNE Rep. No. 51.WCRP Report No.4/2021. July 2021, WMO, Geneva. pp. 9-03-9-04.

Wada, A., S. Kanada, and H. Yamada (2018). Effect of air–sea environmental conditions and interfacial processes on extremely intense typhoon Haiyan (2013). Journal of Geophysical Research: Atmospheres, 123, 10379-10405.

Rainfall simulations of Typhoon Mangkhut (2018) landfalling in the Philippines

Akiyoshi Wada

[1]Meteorological Research Institute, Tsukuba, Ibaraki, 305-0052, JAPAN

[1]awada@mri-jma.go.jp

1. Introduction

Typhoon Mangkhut (2018) was generated around the Marshall Islands (12.7°N, 165.4°E) at 12 UTC on 7 September according to the Regional Specialized Meteorological Center (RSMC) Tokyo best track data. It moved westward and the central pressure reached 905 hPa at 12 UTC on 11 September. After that, Mangkhut had sustained the minimum central pressure for approximately three days and then made landfall in the Philippines province of Cagayan late on 14 September while keeping the central pressure of 905 hPa. Heavy rains caused by Mangkhut flooded Luzon Island, causing a lot of damage there. In order to investigate the predictability of precipitation caused by Mangkhut, numerical simulations were carried out using a 3-km mesh non-hydrostatic atmospheric model (NHM) and the atmospheric-wave-ocean coupled model (AWO) (Wada et al., 2010, 2018).

2. Experimental design

Table 1 shows a list of numerical simulations. The initial time was 1200 UTC on 9 September 27. As described in the introduction, the NHM and AWO were used for the numerical simulations. The computational domain was 4600 x 2500 km. The number of the vertical layer was 55. The top height was approximately 27 km. The integration time was 144 hours. The time step was 3 seconds for NHM, 18 seconds for the ocean model, and 6 minutes for the ocean surface wave model. The Kain-Fritsch cumulus parameterization (KF) (Kain and Fritsch, 1990) was used in order to simulate the precipitation more realistically (Wada and Gile, 2019).

Table1 List of numerical simulations

Name	*Model*	*Cumulus Parameterization*	*Typhoon case and initial time*
NHM	NHM	None	Mangkhut (2018/9/9/1200)
AWO	Coupled NHM-wave-ocean model	None	
NHMKF	NHM	KF	
AWOKF	Coupled NHM-wave-ocean model	KF	

In the experiments AWO and AWOKF, the physical components were exchanged between NHM, the ocean model, and the ocean surface wave model every time step of a model with a longer time step. The Japan Meteorological Agency (JMA) global objective analysis with horizontal resolution of 20 km and the JMA North Pacific Ocean analysis with horizontal resolution of 0.5° were used for creating atmospheric and oceanic initial conditions and atmospheric lateral boundary conditions. The amount of 24-hour accumulated precipitation was calculated by adding up the 0.1°-mesh hourly precipitation obtained from the level-3 standard product of hourly global precipitation dataset of the Global Satellite Mapping of Precipitation (GSMaP: https://sharaku.eorc.jaxa.jp/GSMaP/index.htm) version 04G.

3. Results

3.1 Track and central pressure evolution

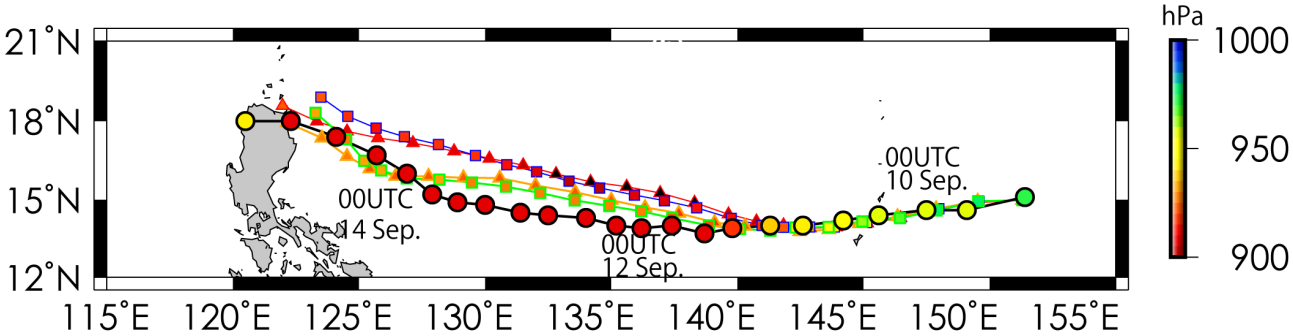

Figure 1 A thick black line with large circles indicates the best track of Mangkhut. Red and orange lines with small triangles indicate the simulation results in the experiments NHM (red) and NHMKF (orange). Blue and green lines indicate the simulation results in the experiments AWO (blue) and AWOKF (green). Colors within the circles indicate the value of central pressure obtained from the RSMC best track data or each experiment.

Figure 1 shows the results of track and central pressure simulations together with the RSMC best track data every 6 hours from 12 UTC on 9 September to 12 UTC on 15 September. The westward movement of Mangkhut analyzed in the best track data is reasonably simulated in all simulations although the northward deflection is obvious. Irrespective of ocean coupling, the northward deflection of simulated track becomes mitigated when the KF parameterization is used. Although the moving speed of simulated Mangkhut is relatively low compared with

that in the best track data, the landfall location is well simulated in the NHMKF and AWOKF simulations

Figure 2 shows the RSMC best-track central pressure evolution together with the simulation results in all experiments. The effect of ocean coupling on the simulated central pressure starts to appear in the intensification phase of Mangkhut on 10 September. In the experiments NHM and AWO, the values of simulated central pressure are comparable to those of best-track central pressure. In the experiments NHMKF and AWOKF, however, the values of simulated central pressure are approximately 20 hPa higher at 12 UTC on 12 September than those in the experiments NHM and AWO although the track simulations become better in the experiments NHMLF and AWOKF.

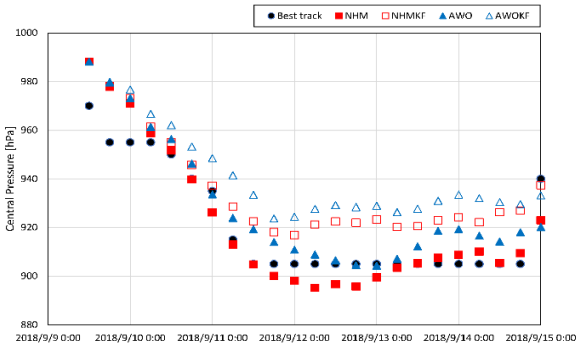

Figure 2 The evolution of RSMC best-track central pressure and simulated central pressures in the experiments NHM, AWO, NHMKF, and AWOKF.

3.2 24-h accumulated precipitation

Figure 3a shows a horizontal distribution of 24-hour accumulated precipitation on 12 September obtained from GSMaP data. The 24-hour accumulated precipitation was calculated by summation of hourly precipitation data. The amount of 24-h accumulated precipitation exceeds 200 mm near the track of Mangkhut. In addition, the area of 24-h accumulated rainfall exceeding 10 mm extends from north (~18 °N) to south (~10 °N). In the experiment AWO, the area over 200 mm shifts eastward because of slow translation of simulated Mangkhut (Fig. 3b). In addition, the area of 24-hour accumulated rainfall is meridionally narrower than that obtained from GSMaP. In the experiment AWOKF, the noise-like fine rainfall distribution is removed/smoothed due to the effect of KF (Fig. 3c). The eastward shift of the area over 200 mm caused by the slow translation in the experiment AWO is not seen in the experiment AWOKF. It is probably because of less northward shift of simulated track in the experiment AWOKF (Fig. 1).

It should be noted that the impact of ocean coupling on the horizontal distribution of 24-hour accumulated precipitation is small (not shown). This implies that excessive precipitation along the track of Mangkhut and relatively small precipitation in the surrounding indicate the necessity of the improvement of cloud physics and cumulus parameterization to simulate the precipitation distribution of the typhoon more accurately.

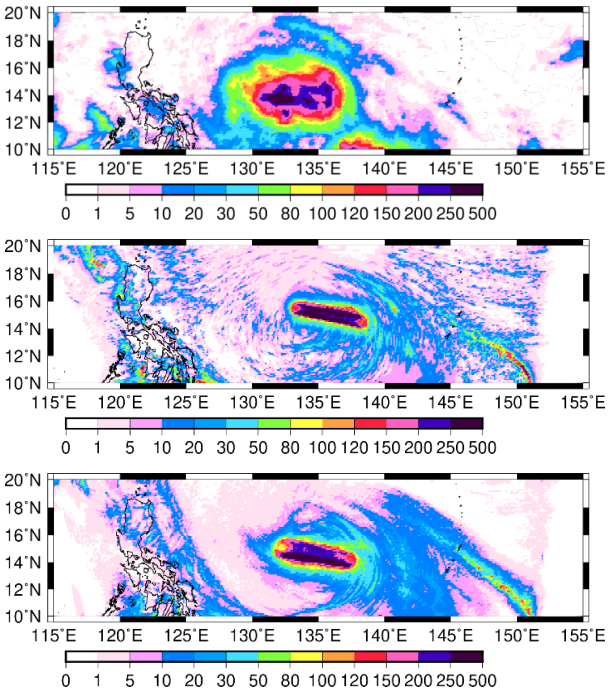

Figure 3 Horizontal distributions of 24-hour accumulated rainfall calculated by summation of hourly rainfall data from 00 UTC to 23 UTC on 12 September obtained from (a) GsMAP, (b) the experiment AWO, and (c) the experiment AWOKF.

4. Ongoing work

The final goal of this study is to improve the accuracy of simulation of precipitation when typhoons make landfall in the Philippines. In situ rainfall observations in the Philippines are needed to investigate the predictability of heavy precipitation caused by typhoons during the landfalling. Moreover, it is necessary to improve the track prediction of typhoons to validate simulation results with in-situ observations. The result in this report shows that the key physical process for both rainfall simulation and improvement of typhoon track prediction is a cumulus parameterization. Tuning the parameter in the cumulus parameterization will be one of the challenging works for simulating Mangkhut more accurately.

References

Kain, J. S., and J. M. Fritsch (1990). A one-dimensional entraining/detraining plume model and its application in convective parameterization. Journal of the Atmospheric Sciences, 47, 2784-2802.

Wada, A., N. Kohno and Y. Kawai (2010). Impact of wave-ocean interaction on Typhoon Hai-Tang in 2005. SOLA, 6A, 13-16.

Wada, A. and R.P.Gile (2019). Roles of ocean coupling and cumulus parameterization in predicting rainfall amounts caused by landfalling typhoons in the Philippines. Research activities in atmospheric and oceanic modelling. CAS/JSC Working Group on Numerical Experimentation. Report No. 49. WCRP Report No.12/2019. WMO, Geneva, pp. 9.07-9.08.

Wada, A., S. Kanada, and H. Yamada (2018). Effect of air–sea environmental conditions and interfacial processes on extremely intense typhoon Haiyan (2013). Journal of Geophysical Research: Atmospheres, 123, 10379-10405.

Development of UFS Coupled Model Infrastructure

Jun Wang[1*], Denise Worthen[2], Bin Li[2], Minsuk Ji[2], Brian Curtis[2], Dusan Jovic[2], Dom Heinzeller[3], Linlin Pan[3], Shrinivas Moorthi[1], Shan Sun[4], Benjamin W. Green[45], Mariana Vertenstein[6], Anthony Craig[7], Gerhard Theurich[8], Rahul Mahajan[1], Arun Chawla[1]

[1]NOAA/NWS/NCEP/EMC, [2]IMSG@NOAA/NWS/NCEP/EMC, [3]DTC-NOAA/GSL-CIRES, [4]NOAA/OAR/GSL, [5]CIRES,University of Colorado, [6]NCAR, [7]STC, [8]ESMF/NRL/SAIC

[*]Jun.Wang@noaa.gov

Introduction:

The Unified Forecast System (UFS) is a community-based coupled Earth system model. It is designed to be the source system for NOAA's operational numerical weather prediction applications. Currently, the UFS can support a range of applications from a standalone atmosphere to several coupled configurations with different combinations of subcomponents at different resolutions. NCEP plans to use UFS coupled configurations in its next global forecast system (GFS) and sub-seasonal to seasonal prediction system (S2S) implementations. In this paper, we describe several major model infrastructure developments that enhance the UFS coupled model forecast capability.

Model description

The latest UFS consists of atmosphere, ocean, sea-ice, wave and data atmosphere models. The atmosphere component consists of the Finite-Volume Cubed-Sphere Dynamical Core (FV3), the Common Community Physics Package (CCPP) and the write grid components. The ocean component is the Modular Ocean Model (MOM6). The Consortium Model for Sea-Ice (CICE) version 6 was recently transitioned into the UFS. The wave model is NOAA's WAVEWATCH III (WW3). The data atmosphere (DATM) is the NEMS data atmosphere model (NEMSDATM). These components are coupled through the Community Mediator for Earth Prediction Systems (CMEPS) within the NOAA Environmental Modeling System (NEMS) infrastructure. Six coupled model benchmark experiments have been conducted at 0.25 degree resolution for a 35-day integration and the results have been verified against observations and analysis data.

Model infrastructure improvements

Three major infrastructure improvements have been made to the UFS coupled model. They are described below.

1. Major model component development

In the atmosphere component, the CCPP [CCPP documentation, 2021] was adopted. This gives the UFS coupled runs the flexibility to choose different atmosphere physics packages. New physics updates from the GFSv16 implementation were merged to the ufs-weather-model repository, which include an updated sa-TKE-EDMF planetary boundary layer scheme, new parameterization in the subgrid scale nonstationary gravity wave drag scheme, updated GFDL microphysics scheme for computing ice cloud effective radius and an updated Noah land surface model. To resolve the issue of inconsistent land/sea masks between atmosphere and ocean grids, a fractional land sea mask capability was added to the atmosphere component. The fractional grid allows water and land to coexist at coastline points. The coupling strategy was also extended so the model can represent air-sea interactions precisely.

The mediator component of the UFS coupled system was transitioned from the NEMS mediator to the Community Mediator for Earth Prediction Systems (CMEPS) [CMEPS documentation, 2020]. CMEPS was developed as a NUOPC-compliant mediator based on ESMF to couple earth sub-components. It extends the NEMS mediator coupling capabilities and is shared by several earth modeling systems, including the Community Earth System Model (CESM) and the Hurricane Analysis and Forecast System (HAFS). The UFS weather model was transitioned to CMEPS from the NEMS mediator to take advantage of the new features developed in CMEPS.

Until recently, the UFS used CICE5 as its sea ice subcomponent. The CICE version 6.0.0 [Hunke, *et al*., 2020] was released in March 2018 with new features including the new icepack version 1.1.0 [Hunke, *et al.*, 2020], enhanced rheology options, dynamic array allocation, and a simplified initialization procedure, etc. The UFS sea ice model was transitioned to CICE6 in August 2020. It was verified that CICE6 and CICE5 perform similarly when both use the same variable freezing temperature method.

A data atmosphere model was added to UFS to support the Global Ocean Data Assimilation System (GODAS). It was found that the SST was increasing during model integration when the DATM was first implemented in DATM-MOM6-CICE5 configuration. The issue was fixed by correcting the bulk formula flux calculations at open water grid points in the mediator. The updated model (DATM-MOM6-CICE6-CMEPS) runs stably in GODAS experiments.

Because the mediator initial conditions are missing in the coupled runs with a concurrent run sequence, a two-step cold start was adopted in the UFS coupled model early benchmarks. A new ocean lag approach was implemented that did not advance the ocean until the second coupling timestep, at which time it advanced two steps. This one step cold start simplifies the cold start process and the differences between the two step and the one step cold start are nearly zero after 12 hours.

2. Build system, repository update and porting

CMake is an open-source compilation tool that provides cross-platform support, improves portability and requires less maintenance. The UFS switched from GNU Make to CMake to take advantage of these new features in October 2020.

A unified repository can avoid issues of inconsistent subcomponents shared by several repositories. It also simplifies the testing process across all the applications. Three UFS application repositories ufs-weather-model, ufs-s2s-model and DATM-MOM6-CICE5 were merged to one unified repository (ufs-weather-model) in September 2020. The unified repository provides a code base for short-range regional weather forecasts, medium-range global weather forecasts and subseasonal to seasonal climate forecasts. This is a critical step toward reducing the number of operational models.

The UFS was ported to several NOAA RDHPCS and other HPC platforms that can be accessed by research communities and universities, and it can also be built and run on laptops and desktops.

3. Regression test update and performance tuning

Several different resolution coupled tests were set up in the UFS regression test suite including 0.25degree (C384MX025), 0.5 degree (C192MX050) and 1.0 degree (C96MX100) runs. In those tests, consistent land sea masks on atmosphere and ocean/ice grids were created in order for the model to run stably. In addition to the regression test, stability tests with benchmark cases of 35-day forecast runs were set up. These tests also work as templates to test new or different physics packages. Restart reproducibility is critical for long climate runs to maintain consistent results. Restart reproducibility without the wave component was maintained when new features were added to the coupled run. Experiments were conducted to tune the number of tasks assigned to each component to achieve load balancing in the coupled runs.

Future work

The model infrastructure development will continue to improve the couple model forecast capability for the next operational implementation at NCEP. Future work includes: 1) setting up a fully coupled system with atmosphere, ocean, sea ice, wave and aerosols through CMEPS; 2) transitioning to the Community Data Models for Earth Predictive Systems (CDEPS) to support other data models including ocean, sea ice and land; 3) merging the Hurricane Analysis and Forecast System (HAFS) application into the UFS repository; 4) updating and maintaining regression tests, setting up CI/CD and cloud support for the coupled model; and 5) improving coupled model computational performance to meet the operational requirements.

References

CCPP v5 technical documentation, 2021: https://ccpp-techdoc.readthedocs.io/en/v5.0.0/

CMEPS documentation, 2020: https://escomp.github.io/CMEPS/versions/master/html/index.html

Elizabeth Hunke, Richard Allard, David A. Bailey, Philippe Blain, Anthony Craig, Frederic Dupont, … Michael Winton. (2020, December 18). CICE-Consortium/CICE: CICE Version 6.1.4 (Version 6.1.4). Zenodo. http://doi.org/10.5281/zenodo.4359860

Elizabeth Hunke, Richard Allard, David A. Bailey, Philippe Blain, Anthony Craig, Frederic Dupont, … Michael Winton. (2020, December 18). CICE-Consortium/Icepack: Icepack 1.2.4 (Version 1.2.4). Zenodo. http://doi.org/10.5281/zenodo.4358418